DESY 03–075
June 2003

arXiv:hep-ph/0306279 v2 2 Aug 2003

On solutions of the Balitsky-Kovchegov equation with impact parameter

K. Golec–Biernat[a,b] and A. M. Staśto[c,a]

[a] *Institute of Nuclear Physics, Radzikowskiego 152, Kraków, Poland*
[b] *II. Institut für Theoretische Physik, Universität Hamburg, Germany*
[c] *DESY, Theory Division, Notkestrasse 85, 22603 Hamburg, Germany*

(August 2, 2003)

Abstract

We analyze numerically the Balitsky-Kovchegov equation with the full impact parameter dependence b. We show that due to the particular b-dependence of the initial condition the amplitude decreases for large dipole sizes r. Thus the region of saturation has a finite extension in the dipole size r, and its width increases with rapidity. We calculate the b-dependent saturation scale and discuss limitations on geometric scaling. We also demonstrate the instant emergence of the power-like tail in impact parameter, which is due to the long range contributions. Thus the resulting cross section violates Froissart bound despite the presence of a nonlinear term responsible for saturation.

1 Introduction

The high energy limit of QCD is one of the most intriguing aspects of hadronic physics. With the advent of new generation accelerators like HERA, Tevatron, RHIC and in a near future LHC, the basic problems of strong interactions are experimentally studied and confronted with theoretical predictions of high energy QCD. The important discovery of the rise of the proton structure functions at HERA [1] at small values of the Bjorken variable x (which is equivalent to the high energy limit) is an example of such a confrontation. This rise was predicted by high energy QCD [2] and is related to the increase of the gluon density. Ultimately the rise has to be damped by the presence of the saturation effects which enter via nonlinear modification to the QCD evolution as first proposed in the pioneering work [3]. Thus QCD at high energy is the theory of high density systems of colored particles. In such systems hard scales appear which allow to apply perturbative techniques although effective interactions in the dense partonic system are of non-perturbative origin. The interplay between hard and soft (perturbative and non-perturbative) aspects of QCD, which also touches in the operational way the issue of confinement, is the most exciting element of high energy QCD.

The effective theory which describes high energy scattering in QCD is Color Glass Condensate [4]. The basic equations of this theory [5] are equivalent [6] to the hierarchy of equations derived by Balitsky [7] and later on reformulated in a compact form by Weigert [8]. These equations contain the BFKL evolution and also the triple Pomeron vertex [9]. In this work we present the results of numerical studies of these basic equations. To be precise we study the simplified version of the hierarchy of Balitsky's equations which reduces to one equation in the limit of large number of colors. This is the equation obtained by Kovchegov [10] in the dipole approach [11] to high energy scattering in QCD. With this equation the deep inelastic lepton–nucleus scattering can be described and also information on small-x hadronic wave function be obtained.

We study this equation in the full form, including the impact parameter dependence b. Previous analytical [12, 13] and numerical [14, 15, 16] studies were done under a simplified assumption of infinitely large and uniform nucleus, i.e. neglecting impact parameter b. Recently, an approximate solution to this equation in semiclassical approach was considered [17]. As we will show, the solutions of the full form of the Balitsky-Kovchegov (BK) equation possess important new features in comparison to the uniform case, e.g. restricted scaling properties with impact parameter dependent saturation scale. The detailed analysis of the $b-$dependence of the solution allows to study the high energy behaviour of the $\gamma^* N$ cross section. We show that the Froissart bound [18] is violated due to the long range contributions in the kernel [19] which brings the issue of the lack of confinement effects in the BK equation. The problem of the Froissart bound was also extensively discussed in the same context in [19, 20] based on analytical consideretations.

The paper is organised in the following way. In the next section we briefly present the BK equation and its symmetries. In Sec. 3 we describe the numerical methods of finding the solution and discuss the initial condition. In Sec. 4 we present the resulting amplitude N as a function of dipole size r and extract the b - dependent saturation scale. In Sec. 5

we discuss the form of the impact parameter profile which emerges in the evolution, and in particular we concentrate on the emergence of the power tails in b in the amplitude. We also present the estimate of the cross section of the black disc radius and its dependence on the rapidity. Finally, in Sec. 6 we state our conclusions.

2 The Balitsky-Kovchegov equation

The deep inelastic scattering of a lepton on a nucleus at high energy in the dipole picture [11, 21] is viewed in the nucleus rest frame as the splitting of an exchanged virtual photon into a $q\bar{q}$ dipole and the subsequent interaction of the dipole with the nucleus. The latter process is described by the dipole-nucleus scattering amplitude $N(\mathbf{x},\mathbf{y})$, where $\mathbf{x},\mathbf{y}$ are two-dimensional vectors of the transverse position of the dipole ends. Alternatively, one can introduce the dipole vector $\mathbf{r}=\mathbf{x}-\mathbf{y}$, and the impact parameter $\mathbf{b}=(\mathbf{x}+\mathbf{y})/2$. Thus in general, the amplitude depends on the four transverse degrees of freedom and rapidity, $Y=\ln(1/x)$, playing the role of the evolution parameter

$$N(\mathbf{x},\mathbf{y},Y) \equiv N_{\mathbf{xy}}(Y)\,. \tag{1}$$

From now on, for shortness of the notation, we assume the $Y-$dependence implicit.

In the leading logarithmic approximation, the dipole scattering amplitude obeys a nonlinear evolution equation derived by Balitsky and Kovchegov [7, 10]

$$\frac{\partial N_{\mathbf{xy}}}{\partial Y} = \overline{\alpha}_s \int \frac{d^2\mathbf{z}}{2\pi} \frac{(\mathbf{x}-\mathbf{y})^2}{(\mathbf{x}-\mathbf{z})^2(\mathbf{y}-\mathbf{z})^2} \left\{N_{\mathbf{xz}} + N_{\mathbf{yz}} - N_{\mathbf{xy}} - N_{\mathbf{xz}}\,N_{\mathbf{yz}}\right\}\,, \tag{2}$$

where $\overline{\alpha}_s = \alpha_s N_c/\pi$. In addition, one has to specify an initial condition at $Y=Y_0$: $N_{\mathbf{xy}} = N^0(\mathbf{r},\mathbf{b})$. The amplitude $N(\mathbf{x},\mathbf{y})$ in (2) is given by the following correlator

$$N(\mathbf{x},\mathbf{y}) = \frac{1}{N_c}\mathrm{Tr}\left\langle 1 - U^\dagger(\mathbf{x})U(\mathbf{y})\right\rangle\,, \tag{3}$$

where the trace is done in the colour space, and the eikonal factor U is defined as the path ordered exponential with the $SU(N)$ gauge fields (in the gauge $A_a^- = 0$)

$$U(\mathbf{x}) = P\,\exp\left\{i\int dx^-\,T^a A_a^+(x^-,\mathbf{x})\right\}\,. \tag{4}$$

The averaging $\langle ...\rangle$ in (3) is performed over an ensemble of classical gauge fields. In general, an infinite hierarchy of equations is found for correlators of the U factors [7]. In the large N_c limit, however, the closed form (2) can be found for the two point amplitude $N_{\mathbf{xy}}$ [10]. The linear part of (2) corresponds to the dipole version [11] of the BFKL equation [22] at nonzero impact parameter and its solution has been studied in the Monte Carlo simulation of onium-onium scattering [23, 24]. The additional quadratic term emerges due to the summation of the multiple interactions of the dipoles in the quark-antiquark wave function with the nucleus.

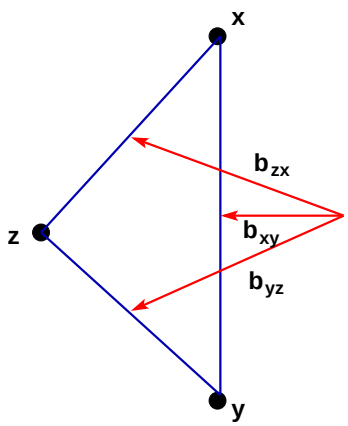

Figure 1: The triangle geometry in Eq. (2). The points $\mathbf{x}, \mathbf{y}, \mathbf{z}$ are the dipole ends in the transverse space, and the vectors $\mathbf{b_{xz}}, \mathbf{b_{xy}}, \mathbf{b_{zy}}$ are the impact parameters of the three dipoles.

The r.h.s of Eq. (2) has a nice geometrical interpretation: the parent dipole $(\mathbf{x}, \mathbf{y})$ splits into two new dipoles $(\mathbf{x}, \mathbf{z})$ and $(\mathbf{y}, \mathbf{z})$, and the summation is taken over all new dipoles. On the other hand, the nonlinear term describes the recombination of the two dipoles $(\mathbf{x}, \mathbf{z})$ and $(\mathbf{y}, \mathbf{z})$ into one $(\mathbf{x}, \mathbf{y})$. The three dipoles form a triangle, shown in Fig. 1. The first part of the integral kernel in (2) only depends on the triangle sides: $|\mathbf{x}-\mathbf{y}|$, $|\mathbf{x}-\mathbf{z}|$ and $|\mathbf{y}-\mathbf{z}|$. A nontrivial dependence on the position of the triangle in the plane, i.e. the dependence on the impact parameter vectors $\mathbf{b_{xy}}, \mathbf{b_{zx}}, \mathbf{b_{yz}}$, is introduced through the arguments of the amplitudes N. In particular, it is interesting to study how the b-dependence introduced by an initial condition $N^0(\mathbf{r}, \mathbf{b})$ propagates with increasing Y. Let us also note that the singularities at $\mathbf{z} = \mathbf{x}, \mathbf{y}$ in Eq. (2) are integrable provided

$$\lim_{\mathbf{x}\to\mathbf{y}} N_{\mathbf{xy}} \sim |\mathbf{x}-\mathbf{y}|^{\epsilon}, \qquad \epsilon > 0\,. \tag{5}$$

Thus the dipole which shrinks to a point does not scatter.

2.1 Symmetries of the BK equation

The BK equation (2) has a rich symmetry structure. Introducing the complex number notation for the transverse vectors, e.g. $x = x_1 + i\,x_2$ and $\overline{x} = x_1 - i\,x_2$ for $\mathbf{x} = (x_1, x_2)$, it can be easily shown that the measure in Eq. (2),

$$\frac{\overline{\alpha}_s}{2\pi}\,\frac{(\mathbf{x}-\mathbf{y})^2}{(\mathbf{x}-\mathbf{z})^2(\mathbf{y}-\mathbf{z})^2}\,d^2\mathbf{z}\,, \tag{6}$$

is invariant under the Möbius transformation[1]

$$x \to \frac{a\,x+b}{c\,x+d}\,, \qquad \overline{x} \to \frac{\overline{a}\,\overline{x}+\overline{b}}{\overline{c}\,\overline{x}+\overline{d}}\,, \tag{7}$$

[1]Provided $\overline{\alpha}_s$ is kept constant.

where the parameters $a, b, c, d \in \mathbb{C}$ and $ad - bc \neq 0$. Identical transformations are also applied to y ($\overline{y}$) and z ($\overline{z}$). Thus the BK equation is *covariant* with respect to the Möbius transformation. In particular, the following elementary transformations from (7) are relevant for our discussion

- global two-dimensional translations by vectors $\mathbf{b}$: $\mathbf{x} \to \mathbf{x} + \mathbf{b}$,
- global two-dimensional rotations by angles ϕ: $\mathbf{x} \to O(\phi)\,\mathbf{x}$,
- scale transformations with a real, positive parameter λ: $\mathbf{x} \to \lambda\,\mathbf{x}$
- inversion (in complex notation): $x \to 1/x$.

Notice, that if an initial condition N^0 is invariant under any of the discussed transformations, the solution of the BK equation $N_{\mathbf{xy}}(Y)$ preserves the corresponding symmetry. In particular, if an initial condition is invariant under translations and rotations, $N(\mathbf{x}, \mathbf{y}) = N^0(|\mathbf{x} - \mathbf{y}|)$, the solution at any rapidity Y has the same property, i.e. it only depends on the dipole size $r = |\mathbf{x} - \mathbf{y}|$ but not on the impact parameter $\mathbf{b} = (\mathbf{x} + \mathbf{y})/2$. The problem of finding solution simplifies enormously in this case since only one degree of freedom is relevant, namely the dipole size r.

Physically, this approximation (called *local approximation*) corresponds to an infinitely large and uniform nucleus. Previous analytical [12, 13] and numerical [14, 15, 16] studies of the BK equation were based upon this assumption. In this approximation, the solution shows saturation, $N(r) \to 1$, with the characteristic scale $Q_s(Y)$. For dipoles smaller than the inverse of the saturation scale, $r < 1/Q_s(Y)$, the solution is governed mainly by the linear term of Eq. (2) and shows the exponential rise in rapidity, $N \sim \exp(\omega_{I\!P} Y)$ where $\omega_{I\!P} = 4 \ln 2\, \overline{\alpha}_s$ is the intercept of the BFKL kernel. On the other hand, in the region where dipoles are large, $r > 1/Q_s(Y)$, the nonlinear term slows down the rise and eventually the amplitude saturates to 1. The saturation scale $Q_s(Y)$ depends on the rapidity in the following way [12, 13, 14, 16, 25]

$$Q_s(Y) \;=\; Q_0 \exp(\lambda\, \overline{\alpha}_s Y)\,, \tag{8}$$

where the coefficient[2] $\lambda \simeq 2$. The solution in the local approximation also exhibits a property of the *geometric scaling* [26], namely for $r > 1/Q_s(Y)$

$$N(r, Y) \;\equiv\; N(r Q_s(Y))\,, \tag{9}$$

which means that the amplitude N in the saturated region only depends on one combined variable $r Q_s(Y)$ instead of r and Y separately[3]. Thus the diffusion into infrared, typical for the linear BFKL equation, is damped by the emergence of the saturation scale $Q_s(Y)$ [16].

[2] To be precise in Ref. [12] the coefficient was found to be the same as the Pomeron intercept $\lambda = \omega_{I\!P}/\overline{\alpha}_s = 4 \ln 2$, but this value was not confirmed by subsequent analytical and numerical studies.

[3] This is also a feature of the saturation model [27].

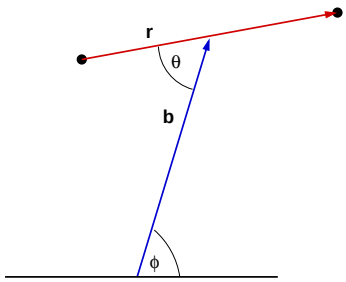

Figure 2: Dipole degrees of freedom: the dipole vector $\mathbf{r}$ and the impact parameter $\mathbf{b}$.

Since in our analysis we want to study the impact parameter dependence, we obviously have to abandon the assumption about the translational invariance. However, in order to simplify the problem, we adopt more physical assumption that our nucleus is cylindrically symmetric, i.e. $N(\mathbf{x},\mathbf{y})$ is invariant under the global rotation. It means that in the parameterisation of the dipole position, see Fig. 2,

$$(\mathbf{x},\mathbf{y}) \,=\, (r, b, \theta, \phi)\,, \tag{10}$$

we drop the dependence on the azimuthal angle ϕ. Note that we keep the dependence on θ which is the angle between the vectors $\mathbf{r}$ and $\mathbf{b}$

$$\cos\theta \,=\, \frac{\mathbf{r}\cdot\mathbf{b}}{r\,b}\,. \tag{11}$$

The assumption about cylindrical symmetry reduces the number of parameters in the amplitude N to four: three degrees of freedom for a dipole and the evolution variable Y.

3 The numerical method of finding solution

The numerical method for the solution of the BK equation is very similar to the one used for the solutions of the linear equations, see [28]. We discretise the amplitude $N(r, b, \cos\theta)$ in all 3 variables $(\ln r, \ln b, \cos\theta)$. A simple linear interpolation has been chosen which is the fastest in this case. To find the solution as a function of rapidity we take in the first step N^0, the initial condition at $Y = Y_0$, and evaluate Eq. (2) with the step ΔY. This gives the first approximation for the solution at $Y = \Delta Y$

$$N^{(1)}_{\mathbf{xy}} \,=\, N^0_{\mathbf{xy}} + \Delta Y \int_{\mathbf{z}} \{N^0_{\mathbf{xz}} + N^0_{\mathbf{yz}} - N^0_{\mathbf{xy}} - N^0_{\mathbf{xz}} N^0_{\mathbf{yz}}\ ,\} \tag{12}$$

where we symbolically denoted the integration over $\mathbf{z}$ with the measure (6). If the relative difference $|(N^{(1)}_{\mathbf{xy}} - N^0_{\mathbf{xy}})/N^0_{\mathbf{xy}}| < \epsilon$ (some accuracy) at each point of the grid, we finish our

procedure, otherwise solution (12) is used to find the second approximation from:

$$N^{(2)}_{\mathbf{xy}} = N^0_{\mathbf{xy}} + \frac{\Delta Y}{2}\int_{\mathbf{z}} \left[N^0_{\mathbf{xz}} + N^0_{\mathbf{yz}} - N^0_{\mathbf{xy}} - N^0_{\mathbf{xz}} N^0_{\mathbf{yz}}\right] + \frac{\Delta Y}{2}\int_{\mathbf{z}} \left[N^{(1)}_{\mathbf{xz}} + N^{(1)}_{\mathbf{yz}} - N^{(1)}_{\mathbf{xy}} - N^{(1)}_{\mathbf{xz}} N^{(1)}_{\mathbf{yz}}\right] + \frac{\Delta Y}{6}\int_{\mathbf{z}} \left[N^{(1)}_{\mathbf{xz}} - N^0_{\mathbf{xz}}\right]\left[N^{(1)}_{\mathbf{yz}} - N^0_{\mathbf{yz}}\right] . \quad (13)$$

The r.h.s. of Eq. (13) was found after integrating over Y from 0 to ΔY, assuming a linear interpolation in Y between N^0 and $N^{(1)}(\Delta Y)$. This is justified for small enough value of ΔY. We iterate in this way, using Eq. (13), until the desired accuracy is achieved.

Usually only couple of iterations are needed to find the right answer, in fact we fix the maximal number of iterations to 5. In order to get satisfactory results one has to work with a grid which is at least $(100_r \times 100_b \times 20_c)$. Each step in rapidity produces about 1.5 MB of output data and takes about 300 min. of CPU time when run on PC machine with 2.5 GHz processor and 2.0 GB RAM memory.

One of the important issues while studying the BK equation is the choice of the initial condition at rapidity $Y = 0$. As mentioned above, because of the cylindrical symmetry our initial amplitude N^0 should only depend on the three variables (r, b, θ). Since we have nearly no information on the angle θ between $\mathbf{r}$ and $\mathbf{b}$, we do not assume any dependence on it in the initial conditions. We shall see that the nontrivial θ dependence is nevertheless generated through the evolution. As far as the r and b dependence is concerned we have chosen the initial distribution in the Glauber–Mueller form [29, 30]

$$N^0(r, b) = 1 - \exp\{-r^2 S(b)\} , \quad (14)$$

with $S(b)$ being a steeply falling profile in b, e.g. $S(b) \sim \exp(-b^2)$. The Glauber–Mueller formula resums the multiple scatterings of a single dipole on a nuclear target and it has been advocated to be a natural choice for the starting distribution of the BK equation [10]. Let us note that the above distribution has a property that for any fixed value of impact parameter it saturates to 1 for sufficiently large values of the dipole size r. More detailed analysis with other forms of the initial conditions will be presented elsewhere [31].

4 The dependence of the solution on a dipole size r

We have performed the numerical evolution of the BK equation starting from formula (14) as the initial condition with the following impact parameter profile

$$S(b) = 10 \, \exp\{-b^2/2\} . \quad (15)$$

Throughout this work we keep the coupling constant in (2) fixed, $\overline{\alpha}_s = 0.2$. The running of the coupling, although physically more justified, would be an additional complication

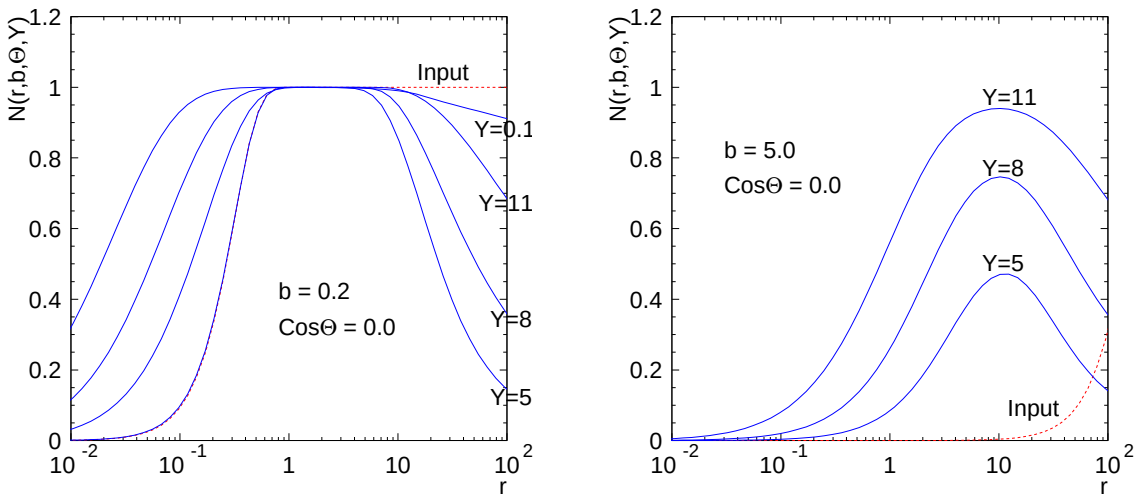

Figure 3: The amplitude $N(r, b, \theta; Y)$ as a function of dipole size r for indicated values of rapidity Y and two values of the fixed impact parameter: $b = 0.2$ (left) and $b = 5$ (right). The orientation of the dipole $\cos\theta = 0$. The red-dashed line is the input distribution (14) with profile (15).

to the solution which we would like to avoid at this stage[4]. Nevertheless, one should stress that a running coupling is an important NLL effect [34], which should be taken into account in future investigations. We are going to study now how such initial condition (14) is modified by the evolution in rapidity. We concentrate first on the dependence of the solution on a dipole size r.

The results of our numerical analysis are shown in Fig. 3 for two values of the impact fixed impact parameter: $b = 0.2$ and $b = 5$. We have also fixed the orientation of the dipole such that $\mathbf{r} \perp \mathbf{b}$ that is $\cos\theta = 0$, see Eq. (11). As we see, for the values of r which are small (here $r \ll 1$) the amplitude rises with increasing values of rapidity Y. In this region, the linear part of the BK equation dominates. With increasing r, for fixed rapidity, the amplitude finally reaches the saturation value $N_{\rm sat} = 1$, were the nonlinearity of the BK equation is crucial. This is mostly visible for small value of impact parameter, Fig. 3 (left). For a larger value of impact parameter, $b = 5$, in the plot to the right, the saturation has been only reached for the highest value of rapidity shown $Y = 11$. What is interesting is the fact that the amplitude has a maximum for the dipole size which is twice its impact parameter $r = 2b$, that is $r = 10$ in this case.

At large r, the behaviour of the amplitude is quite different from the case with the translational invariance (no $b-$dependence). The amplitude decreases with increasing r even if the initial condition is saturated ($N^0 = 1$) in this region. The reason for this

[4]In the local approximation, running coupling changes rapidity dependence of the saturation scale: $Q_s^{\rm run}(Y) \sim \exp(c\sqrt{Y})$, see [16, 32, 33] and also [3].

behaviour can be easily understood analysing the solution after the first iteration (12)

$$N^{(1)}_{\mathbf{xy}} \,=\, N^{0}_{\mathbf{xy}} \,+\, \Delta Y\, \frac{\overline{\alpha}_s}{2\pi} \int d^2\mathbf{z}\, \frac{(\mathbf{x}-\mathbf{y})^2}{(\mathbf{x}-\mathbf{z})^2(\mathbf{y}-\mathbf{z})^2}\, \left\{ N^{0}_{\mathbf{zy}} + N^{0}_{\mathbf{xz}} - N^{0}_{\mathbf{xy}} - N^{0}_{\mathbf{xz}}\, N^{0}_{\mathbf{yz}} \right\}\,, \quad (16)$$

with the Glauber-Mueller initial condition

$$N^0(r,b) \,=\, 1 - \exp\{-c\, r^2 \exp(-b^2 d)\}\,. \quad (17)$$

Saturation means that for a large enough $r = |\mathbf{x}-\mathbf{y}|$ (and fixed b) $N_{\mathbf{xy}} \to 1$, i.e. a large dipole is totally absorbed. This is indeed the case for the initial condition (17). After the first evolution step, however, $N^{(1)}_{\mathbf{xy}}$ becomes less than 1 for large r due to the large and negative integrand in the curly brackets in (16), which leads to the effect shown in Fig. 3 at large r.

Indeed, if $N^{0}_{\mathbf{xy}} \simeq 1$ in Eq. (16), the integrand is always negative or equal zero

$$N^{0}_{\mathbf{xz}} + N^{0}_{\mathbf{yz}} - 1 - N^{0}_{\mathbf{yz}} N^{0}_{\mathbf{xz}} \,=\, -(1 - N^{0}_{\mathbf{zy}})(1 - N^{0}_{\mathbf{xz}}) \,\leq\, 0\,. \quad (18)$$

In Fig. 1 we show an example of typical configurations of the $(\mathbf{x},\mathbf{z})$ and $(\mathbf{y},\mathbf{z})$ dipoles which give dominant contribution to the integral in Eq. (16). For such a contribution $r_{xz} \approx r_{yz} \approx 2b_{xz} \approx 2b_{yz} \approx r$ (for $b_{xy} \approx 0$), and for the initial condition (17) the amplitudes $N^{0}_{\mathbf{xz}} \approx N^{0}_{\mathbf{yz}} \approx 0$ for the sufficiently large value of r. Thus the integral picks up significant negative contribution from this configuration. This should be contrasted to the translationally invariant case with no $b-$dependence in the initial condition, e.g. $N^0(r) = 1 - \exp\{-r^2\}$. For such initial condition the configuration from Fig. 1 gives $N^{0}_{\mathbf{xz}} \approx N^{0}_{\mathbf{yz}} \simeq 1$, and the expression in Eq. (18) is negligible. One can prove that any other configuration, for example when $|\mathbf{x}-\mathbf{z}| \ll |\mathbf{x}-\mathbf{y}|$ or $|\mathbf{x}-\mathbf{z}| \gg |\mathbf{x}-\mathbf{y}|$, leads to the same result. Thus, in the case of infinitely large and uniform nucleus, the amplitude N stays always saturated for large dipole sizes.

In the next evolution step, $N^{(1)}_{\mathbf{xy}}$ plays the role of the initial condition. Since $N^{(1)}_{\mathbf{xy}}$ is no longer equal to 1 for large dipole sizes, the analysis becomes more complicated. At some rapidity, the discussed integral becomes positive leading to the effect observed in Fig. 3 where N starts to grow again, reaching unity at large r for large values of rapidity.

In more physical terms the fall-off of the amplitude at large r can be explained by realizing that the end points $\mathbf{x}$ and $\mathbf{y}$ of a sufficiently large dipole are in the region where there is no gauge field. In this case $U(\mathbf{x}) = U(\mathbf{y}) = 1$, and the correlator (3) vanishes. It simply means that the dipole is so large that it misses the localised target given by $S(b)$. On the other hand, the non-vanishing value of the amplitude for very large values of r in the previous studies in the local approximation [12, 13, 14, 15, 16] was a consequence of the fact that the field was uniform and present everywhere, thus it did not matter how large the dipole was, it always scattered. The appearance of the gauge field, signalled by the increase of N with rising rapidity, corresponds to expansion of a black (or grey) region of a nucleus, see section 5.3.

4.1 Saturation scale and geometric scaling

The saturation scale Q_s is defined from the condition

$$\langle N(r = 1/Q_s, b, \theta, Y) \rangle_\theta = \kappa \,, \tag{19}$$

where the constant κ is of the order of unity ($\kappa = 1/2$ in our numerical analysis) and we have taken an average over the orientation of the dipole with respect to the vector of impact parameter. Notice that after solving the above equation, the saturation scale depends on impact parameter in addition to rapidity[5]. For the form of N, shown in Fig. 3, there are two solutions of Eq. (19) for sufficiently large rapidities, corresponding to small and large dipole sizes. Thus saturation (defined here as $N > \kappa$) occurs over a finite region of dipole sizes

$$1/Q_s(b, Y) < r < R_H(b, Y) \,. \tag{20}$$

The scale $Q_s(b, Y)$ is the b-dependent saturation momentum introduced by Mueller [30]. The $b-$independent saturation scale found in the previous analyses [13, 14, 15, 16] can be regarded as an average over all area of interaction $Q_s(Y) = \langle Q_s(Y, b) \rangle_b$. The second scale $R_H(b, Y)$ appears because we have introduced exponential impact parameter profile, as has been explained in detail in the previous section, and reflects the boundary of the nucleus. In Fig. 4 we show the form of the impact parameter profile of the saturation scale $Q_s(b, Y)$ for two different rapidities $Y = 5$ and $Y = 11$. The saturation scale at $Y = 0$, shown by the dashed line for comparison, is computed from the initial condition (14) with (15)

$$Q_s^2(b, 0) = Q_0^2 \exp(-b^2/2) \,, \tag{21}$$

where we have fixed the normalisation Q_0 to match the $Q_s(b, Y)$ at small values of $b = 0.1$. Thus the dashed lines in Fig. 4, show the profile of $Q_s(b, Y)$ which we would get if the exponential impact parameter dependence set in the initial conditions would be preserved through the evolution. We clearly see that for higher impact parameters, the exponential fall-off set by initial condition is replaced by the power-like tail $Q_s(b, Y = 11) \sim 1/b^\gamma$ with $\gamma \simeq 1.6 - 2.0$ for $b > 7$.

As it is evident from Fig. 3, both the saturation scale $Q_s(b, Y)$ and $R_H(b, Y)$ rise with increasing rapidity, thus leading to broadening of the region in r for which saturation occurs. The energy dependence of $Q_s(b, Y)$ has been estimated to be proportional to $\exp(\lambda_s \overline{\alpha}_s Y)$ with $\lambda_s \simeq 1.7-2.0$ at the highest values of rapidity $Y = 9-11$. We also checked that this value of λ_s is not very sensitive to impact parameter. This would mean that (at high rapidities) the saturation scale has a factorised form $Q_s(Y, b) = \exp(\lambda_s \overline{\alpha}_s Y)\, g(b)$. We expect exponential dependence on rapidity of $R_H(b, Y) \sim \exp(\lambda_H \overline{\alpha}_s Y)$ too, and we have found $\lambda_H \simeq 2.9$.

Since there are two scales in the problem, Q_s and R_H, geometric scaling of the form (9) is not present anymore for arbitrarily large dipoles. However, when $r \ll R_H(b, Y)$ there is still an approximate geometric scaling in the combined variable $r\, Q_s(b, Y)$ for fixed b.

[5] Of course, Q_s depends also on κ but this dependence is irrelevant for our discussion.

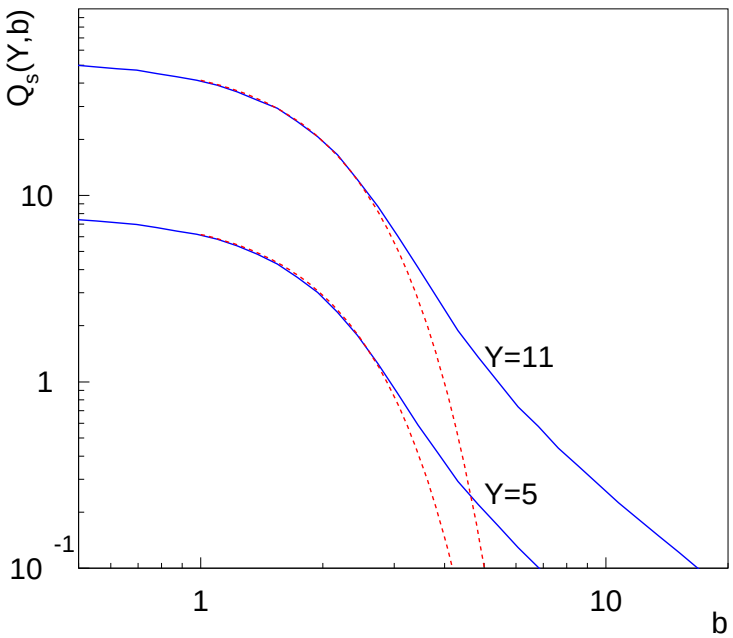

Figure 4: The dependence of the saturation scale $Q_s(b,Y)$ on impact parameter for two fixed values of rapidity. For the comparison the saturation scale at initial rapidity (21) is shown by the dashed line, normalised to the value of $Q_s(b,Y)$ at $b = 0.1$.

This is shown in Fig. 5, obtained from Fig. 3 after rescaling r by $\exp(1.7\,\overline{\alpha}_s Y)$, i.e. by the rapidity dependence of the saturation scale $Q_s(b,Y)$, extracted in the region $7 \leq Y \leq 11$. As discussed, there is no geometric scaling for large dipole sizes. The problem of scaling in the $b-$dependent case has already been addressed in [20] and in recent phenomenological studies [35], and still needs deeper analysis.

Let us finally note that for our solution there is a region in b in which the saturation scale does not exist at all. It is evident from the right hand side plot in Fig. 3, where up to the rapidities $Y \sim 6$ the amplitude $N < \kappa$ for all values of the dipole sizes r, and Eq. (19) does not have a real solution.

5 Impact parameter dependence of the solution

We will discuss now the impact parameter dependence of the solution to the BK equation with the Glauber-Mueller input distribution (14,15).

In Fig. 6 we show the amplitude $N(r,b,\theta;Y)$ as a function of impact parameter b for fixed and small dipole size $r = 0.1$ and various values of rapidity. We have also fixed the orientation of the dipole such that $\cos\theta = 0$. The first striking feature of the solution is

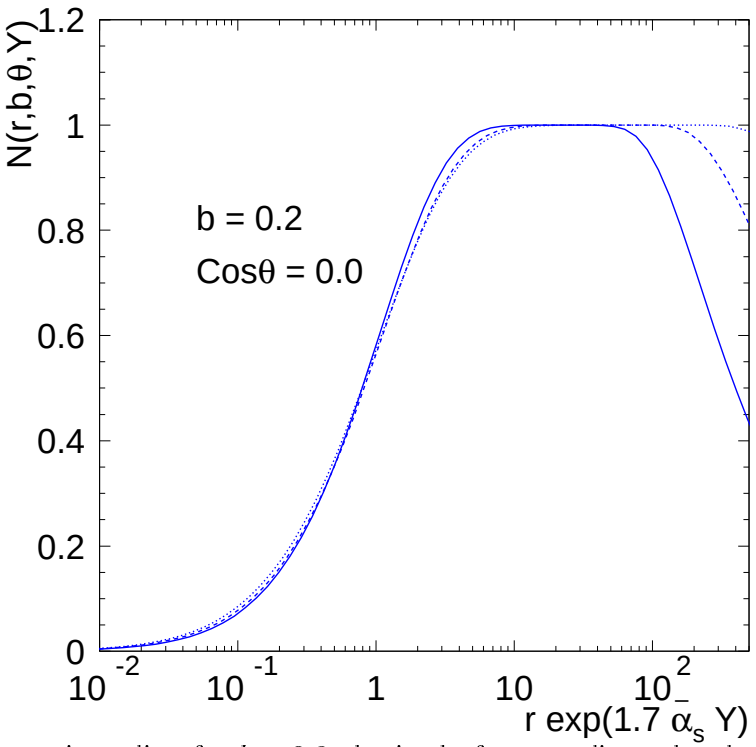

Figure 5: Geometric scaling for $b = 0.2$ obtained after rescaling r by the rapidity dependence of the saturation scale $Q_s(b, Y)$. Dotted, dashed and solid lines are for $Y = 11, 9, 7$ respectively. The orientation of the dipole has been fixed such that $\cos\theta = 0$.

the fact that the steeply falling exponential dependence in b, given by the initial profile $S(b)$, is washed out by the evolution and instead clear power behaviour is generated for large values of b. Initially, at lowest rapidity $\Delta Y = 0.1$ the amplitude $N(b) \sim 1/b^{3.6}$, whereas later on it has a milder dependence: $N(b) \sim 1/b^{\gamma}$ with γ between 2 and 3 for $Y \geq 5$. The growth of the amplitude as a function of rapidity at large impact parameters is exponential, $N(Y) \sim \exp(\omega Y)$ with $\omega \simeq 2.7\,\overline{\alpha}_s$ for $b = 10$. This strong dependence is clearly governed by the linear BFKL part of the equation since the amplitude is small enough for the nonlinear term to be safely neglected and it is in a very good agreement with the hard Pomeron intercept $\omega_{I\!P} = 4 \ln 2\,\overline{\alpha}_s = 2.77\,\overline{\alpha}_s$.

On the other hand, at small values of impact parameters, $b < 1$, where the amplitude is large, we clearly observe that the growth of amplitude is strongly damped due to the nonlinear term. This is the region of b where the saturation sets in first.

5.1 The origin of the power-like tail

It has been argued by Kovner and Wiedeman in [19] that the power behaviour in impact parameter $N \sim 1/b^{\gamma}$ originates from the configurations with very large dipoles. Following [19] let us take small dipole with size $r = |\mathbf{x} - \mathbf{y}|$ which is located far away from the target,

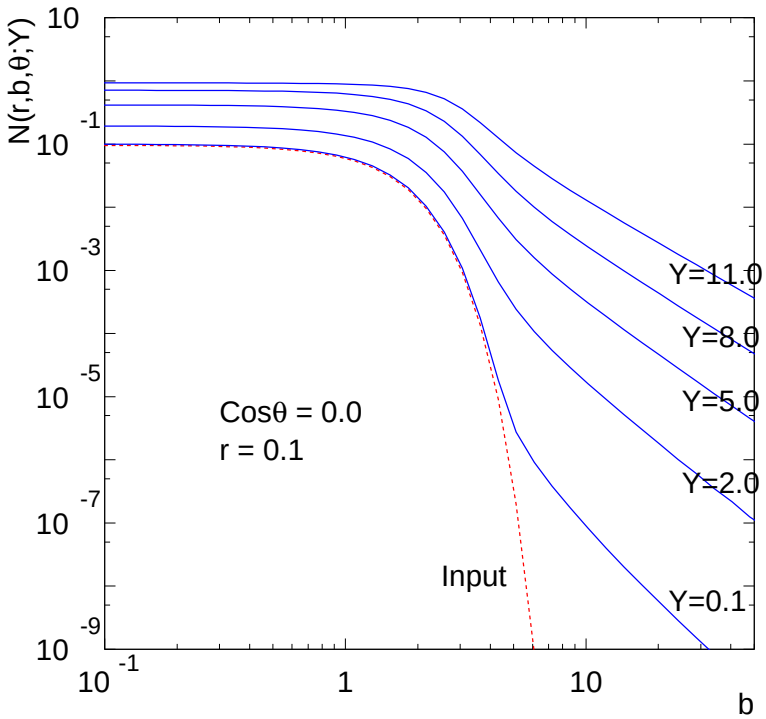

Figure 6: The amplitude $N(r, b, Y)$ as a function of impact parameter b for different values of rapidity Y. The dipole size and orientation are fixed, $r = 0.1$ and $\cos\theta = 0$. The dashed line is the input distribution (14) with the profile (15).

at large impact parameter b, in the area where the colour field is very weak. In that case one has $U(\mathbf{x}) \simeq U(\mathbf{y}) \simeq 1$ and thus $N(\mathbf{x}, \mathbf{y}) \simeq 0$.

The non-vanishing contribution to the r.h.s of equation (2) comes from configurations of large dipoles with one end-point situated at $\mathbf{x}$, and the other at $\mathbf{z}$, close to the center of the target where the field is strong. The phase in eikonal (4) oscillates strongly and thus $\langle U(\mathbf{z}) \rangle \simeq 0$. Therefore $N(\mathbf{x}, \mathbf{z}) \simeq N(\mathbf{y}, \mathbf{z}) \simeq 1$, and this configuration gives

$$\int d^2\mathbf{z}\, \frac{(\mathbf{x}-\mathbf{y})^2}{(\mathbf{x}-\mathbf{z})^2(\mathbf{y}-\mathbf{z})^2}\, (N_{\mathbf{xz}} + N_{\mathbf{yz}} - N_{\mathbf{xy}} - N_{\mathbf{xz}}N_{\mathbf{yz}}) \simeq \frac{r^2}{b^4} \int d^2\mathbf{z} \simeq \frac{r^2}{b^4}\, \pi R_0^2(Y) \quad (22)$$

where $\pi R_0^2(Y)$ is the area of strong field in the target over which we integrate. Strictly speaking the statement that $N(\mathbf{x}, \mathbf{z}) = 1$ for the configuration considered above is valid only at very high rapidities. Due to the initial conditions (14) at intermediate rapidities there will be always such b, large enough, for which these configurations will have $N(\mathbf{x}, \mathbf{z}) < 1$, however always $N(\mathbf{x}, \mathbf{z}) \gg N(\mathbf{x}, \mathbf{y})$.

In order to check this statement numerically we perform only one iteration of the BK equation with very small step in rapidity $\Delta Y = 0.1$, Eq. (12), and divide the integration region into two parts: $|\mathbf{z} - \mathbf{b}| < r_0$ and $|\mathbf{z} - \mathbf{b}| > r_0$ with the cutoff $r_0 = 1$ for the choice

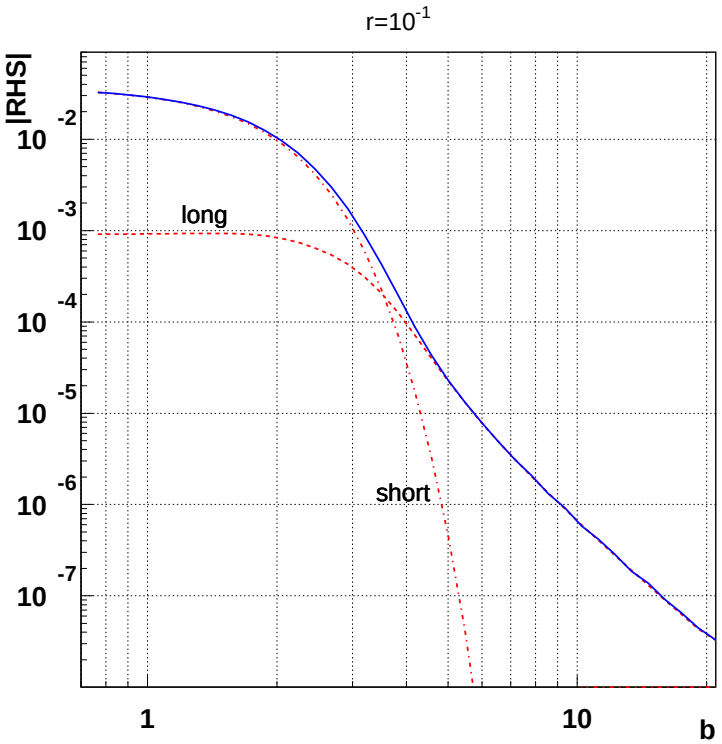

Figure 7: The r.h.s. of the BK equation (2) computed for the initial condition (14,15) (solid line) and the contributions from the short and long dipoles (dashed lines), see (23), plotted as a function of b for fixed dipole size $r = 0.1$ and orientation $\cos\theta = 0$.

of small dipole $r = 0.1$. To be precise we evaluate two integrals:

$$\left[\overbrace{\int \Theta(r_0 - |\mathbf{z}-\mathbf{b}|)}^{short} + \overbrace{\int \Theta(|\mathbf{z}-\mathbf{b}| - r_0)}^{long} \right] \frac{d^2\mathbf{z}\,(\mathbf{x}-\mathbf{y})^2}{(\mathbf{x}-\mathbf{z})^2(\mathbf{y}-\mathbf{z})^2} (N^0_{\mathbf{xz}} + N^0_{\mathbf{yz}} - N^0_{\mathbf{xy}} - N^0_{\mathbf{xz}} N^0_{\mathbf{yz}}) \tag{23}$$

with N^0 being our initial condition. The results are presented in Fig. 7, where the short range contribution dominates at small values of impact parameters and the long range one appears to be responsible for the power behaviour in b at large values. The point at which the long range contribution starts to dominate over the short range one is determined by the form of the initial condition.

5.2 Angular dependence for large dipole sizes

It is interesting to study also the angular dependence of the solution N. For sufficiently small dipole sizes $r \ll R_H$, the angular dependence is negligible. However, when $r \sim R_H$ the difference in the amplitude due to the dipole orientation is quite substantial, especially at large impact parameters $b \sim r$.

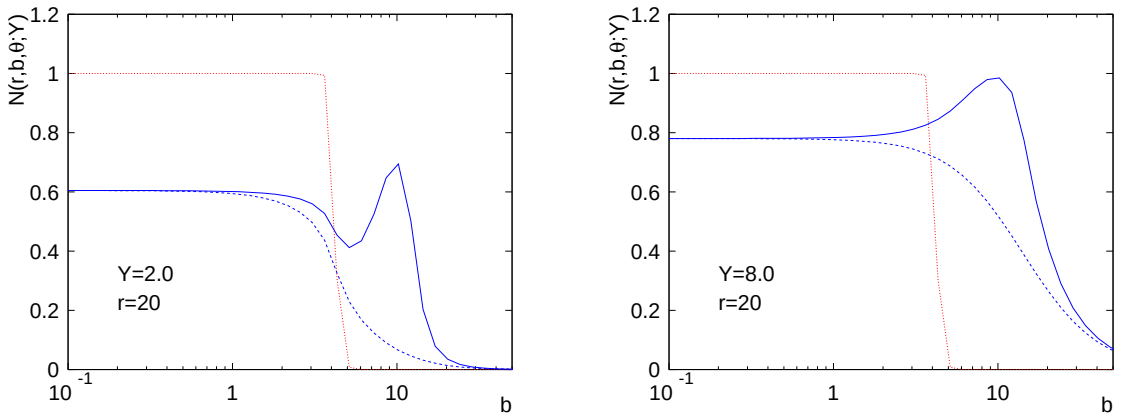

Figure 8: The amplitude $N(r, b, \theta; Y)$ as a function of impact parameter b for two rapidities: $Y = 2$ (left) and $Y = 8$ (right). The dipole size is fixed to $r = 20$. The solid blue line corresponds to the case $\mathbf{r} \,||\, \mathbf{b}$, and for the dashed blue line $\mathbf{r} \perp \mathbf{b}$. The red-dotted line is the input distribution (14) with (15).

In Fig. 8 we plot $N(r, b, \theta; Y)$ as a function of b for a large dipole with $r = 20$. Two rapidities were considered. In both cases we have compared calculation with $\mathbf{r} \,||\, \mathbf{b}$, solid line, and $\mathbf{r} \perp \mathbf{b}$, dashed line (together with the input distribution, dotted line). The calculation with parallel orientation shows a characteristic peak at $b = \frac{r}{2}$. This corresponds to the situation when one end of the dipole, $\mathbf{x}$, is situated in the center of the target where the field is strong $\langle U(\mathbf{x}) \rangle \approx 0$ and the other end, $\mathbf{y}$, is located in the area where the field is very weak $U(\mathbf{y}) \approx 1$. Thus the amplitude $N = \left\langle 1 - U^\dagger(\mathbf{x}) U(\mathbf{y}) \right\rangle / N_c \simeq 1$. On the other hand the large dipole perpendicular to the impact parameter axis has both ends in the region where the field is not so strong and therefore $N(\mathbf{x}, \mathbf{y})_\perp < N(\mathbf{x}, \mathbf{y})_{||}$.

5.3 Black disc radius and unitarity bound

The black disc radius $R_{BD}(r, Y)$ defines the region in the impact parameter space where the amplitude N saturates (for a given dipole size r and rapidity Y). It is defined as the solution of the equation

$$\langle N(r, b = R_{BD}, \theta, Y) \rangle_\theta = \kappa \,, \tag{24}$$

with respect to the impact parameter b. As before in Sec. 4.1 in our analysis we choose $\kappa = 1/2$ and average over the angle θ. Thus the black disc radius is a function of the dipole size and rapidity.

The expansion of the black disc area with increasing Y is very important for the behaviour of the total dipole-nucleus cross section with energy $s \sim s_0 e^Y$,

$$\sigma(\mathbf{r}, Y) = 2 \int d^2\mathbf{b} \, N(\mathbf{r}, \mathbf{b}, Y) \,. \tag{25}$$

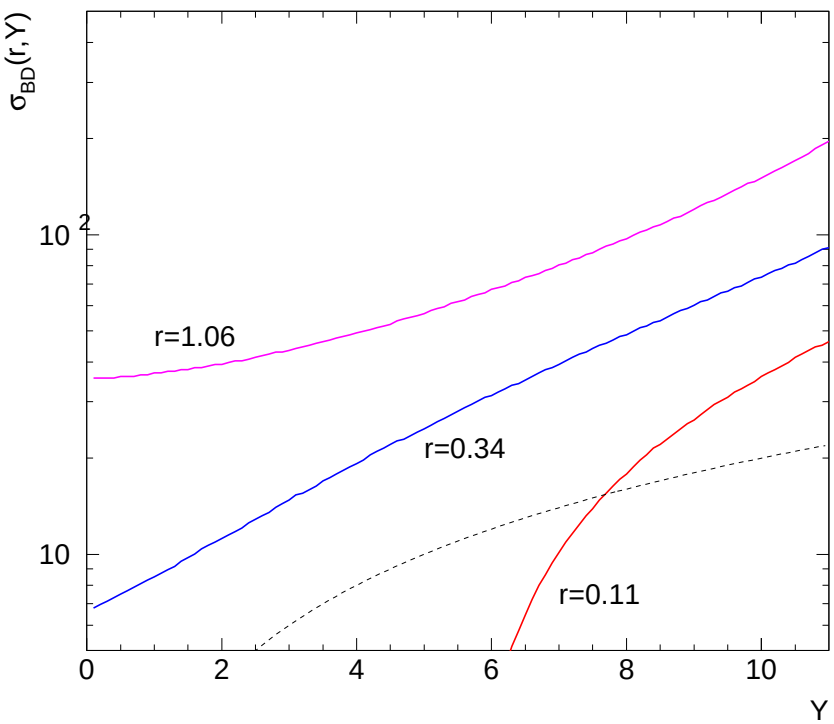

Figure 9: The dipole cross section $\sigma_{BD}(r,Y)$ computed from Eq. (26), plotted as a function of rapidity Y for three different dipol sizes r. The dashed line corresponds to $\sigma_{Test} = c\,Y$.

This cross section is bounded from below by the cross section integrated over the black disc area

$$\sigma_{BD}(\mathbf{r},Y) \;=\; 2\int d^2\mathbf{b}\, N(\mathbf{r},\mathbf{b},Y)\,\Theta(N-\kappa) \;\simeq\; 2\,\pi\, R^2_{BD}(r,Y)\,. \tag{26}$$

Thus the problem of the Froissart bound [18], $\sigma(\mathbf{r},Y) \leq Y^2$ for asymptotically high energies, can be explicitly studied by looking at the rapidity dependence of the black disc radius.

In Fig. 9 we plot σ_{BD} from (26) as a function of rapidity. For the comparison we illustrate the $\sigma_{Test} = c\,Y$ behaviour which would be present if the initial profile in impact parameter $S(b) \sim \exp(-b^2)$ was preserved. Clearly the behaviour of the black disc cross section is much faster than the linear dependence in rapidity. We have found that

$$R_{BD} = R^0_{BD}\exp(\lambda_{BD}\,\overline{\alpha}_s Y)\,. \tag{27}$$

The extracted value of $\lambda_{BD} \simeq 0.6-0.7$ for $r = 0.3-1$ and $\lambda_{BD} \simeq 0.9-1$ for $r = 3-30$ at the highest rapidity $Y = 11$.

The value of λ_{BD} increases rapidly for dipole sizes smaller than the given range above, mostly due to the pre-asymptotic effects. The value of λ_{BD} is smaller than $\lambda_{BD} = 0.87\,\omega_{I\!P}/(2\overline{\alpha}_s) \simeq 1.2$ which was quoted in Ref. [19]. The origin of this discrepancy can be roughly explained by noting that the power given in [19] most probably overestimates the growth of the black disc radius because it was derived from the analysis of the saddle point solution to the linear equation. On the other hand in our numerical simulations the value of $\lambda_{BD} = 0.9 - 1.0$ for large r is probably closer to the asymptotic one. It is due to the fact that for large r, the amplitude has a clear peak for $b = r/2$ which is generated entirely through the evolution. In other words the amplitude in this region is less sensitive to the initial profile in b. It is also interesting that this value λ_{BD} is consistent with the relation $\lambda_{BD} = 1/2\lambda_s$, based on the following argument of the conformal invariance of the equation (see also [36]).

Let us take the saddle point solution to the dipole version of the BFKL equation in the transverse space [37, 23]

$$N(r_0, r, b, Y) \;\sim\; \frac{r r_0}{16 b^2}\frac{1}{Y^{3/2}} \ln\frac{16 b^2}{r r_0} \exp\left(\omega_{I\!P} Y - \ln^2 \frac{r r_0}{16 b^2}\frac{1}{14\zeta(3)\overline{\alpha}_s Y}\right) \;. \tag{28}$$

The amplitude is a function of $r r_0/b^2$ only instead of r, b separately, which is the consequence of the conformal invariance. The conditions for the saturation scale (19) and black disc radius (24) mean that (roughly)

$$\frac{r}{R^2_{BD}(r,Y)} \;=\; \frac{1}{b^2 Q_s(b,Y)} \;\longrightarrow\; \frac{R^2_{BD}(r,Y)}{Q_s(b,Y)} = r b^2 \;. \tag{29}$$

Since in the last equality the right hand side does not depend on the rapidity so should not the left hand side too. This means that if we have $R_{BD} \sim \exp(\lambda_{BD}\overline{\alpha}_s Y)$ and $Q_s \sim \exp(\lambda_s \overline{\alpha}_s Y)$ then

$$\lambda_s \;=\; 2\lambda_{BD} \;. \tag{30}$$

Relation (29) means also that $Q_s \sim \frac{1}{b^2}$, which we have already checked to be approximately true (at least for large values of $b > 7$ see Sec. 4.1) and also $R^2_{BD} \sim r$. We have verified that $R^2_{BD}(r, Y = 11) \sim r^a$ with $a \simeq 0.7$ for $r = 0.1 - 1.0$ and $a \simeq 1.0 - 1.1$ for $r = 5.0 - 10.0$.

Clearly the onset of the exponential behaviour in rapidity proportional to $\exp(\lambda_{BD}\overline{\alpha}_s Y)$, visible in Fig. 9, signals violation of the Froissart bound. This behaviour is a consequence of the power tails in impact parameter $N \sim b^{-\gamma}$, in the same way as the steep exponential profile $\sim \exp(-b^2)$ leads to the linear dependence $\sim Y$ of the cross section, compare the argument of Heisenberg in [38]. The exponential increase of the cross section with rapidity despite the multiple scattering interactions has been also observed in the Monte Carlo study of the amplitude for onium-onium scattering [23].

Since the power-like tail is generated by the long-range contribution, the violation of the Froissart bound is caused by the long-range Coulomb-like interactions [19], which in the reality should be suppressed due to confinement. Thus a modification of the BK equation by confinement effects is necessary.

6 Conclusions

The solution to the BK equation with the b-dependence presented in this paper differs substantially from the one with translational invariance. The most important result is the fact that the exponential profile in b in the initial condition is *not preserved* by the evolution. Instead, the power behaviour is generated for large b's whose origin comes from the structure of the BFKL kernel. Such behaviour leads to the violation of the Froissart unitarity bound despite the presence of a local unitarity at fixed impact parameter. The violation of this bound is caused by non-suppressed long range contribution, i.e. the lack of confinement in the BK equation. This feature of the $b-$dependent amplitude is consistent with numerical studies of onium-onium scattering with multiple scattering of dipoles [23], and with the qualitative analysis of the BK equation [19].

Thus in order to satisfy the Froissart bound through the evolution one would have to modify the evolution kernel in the region of long range contribution in order to incorporate confinement. For example, it is evident from Fig. 7, that the naive cut-off – dropping the second term in the square brackets in Eq. (23) – would do the job. In general, conformal symmetry of the integral kernel in the BK equation has to be broken.

Another interesting feature is the dependence of the solution on the dipole size, which shows that the amplitude is saturated in the limited range of scales: $1/Q_s(b,Y) < r < R_H(b,Y)$. Of course, the true behaviour for large dipole sizes should be modified by the long-distance, confinement physics.

Acknowledgments

We would like to thank Jochen Bartels, Edmond Iancu, Alex Kovner, Jan Kwieciński, Misha Lublinsky, Leszek Motyka, Al Mueller, Misha Ryskin, Gavin Salam and Urs Wiedemann for interesting discussions. K.G-B is grateful to Deutsche Forschungsgemeinschaft for a fellowship. This research was supported by the Polish Committee for Scientific Research grants Nos. KBN 2P03B 051 19, 5P03B 144 20.

References

[1] ZEUS Collab., M. Derrick et al., *Phys. Lett.* **B 316** (1993) 412; *Z. Phys.* **C 65**(1995) 379; *Z. Phys.* **C 72**(1996) 399; *Eur. Phys. J.***C 21** (2001) 443;
H1 Collab., I. Abt et al., *Nucl. Phys.* **B 407** (1993) 515; *Nucl. Phys.* **B 470** (1996) 3; H1 Collab., C. Adloff et al., *Nucl. Phys.* **B 497** (1997) 3; *Eur. Phys. J.***C 13** (2000) 609; *Eur. Phys. J.***C 21** (2001) 33.

[2] L. N. Lipatov, *Sov. J. Nucl. Phys.* **23** (1976) 338;
E. A. Kuraev, L. N. Lipatov and V. S. Fadin, *Sov. Phys. JETP* **45** (1977) 199;
I. I. Balitsky and L. N. Lipatov, *Sov. J. Nucl. Phys.* **28** (1978) 338.

[3] L. V. Gribov, E. M. Levin and M. G. Ryskin, *Phys. Rep.* **100** (1983) 1.

[4] L. McLerran and R. Venugopalan, *Phys. Rev.* **D49** (1994) 2233; *ibid.* **D49** (1994) 3352; *ibid* **D50** (1994) 2225;
J. Jalilian-Marian, A. Kovner, L. McLerran and H. Weigert, *Phys. Rev.* **D55** (1997) 5414; R. Venugopalan, *Acta Phys. Polon.* **B30** (1999) 3731;
E. Iancu, A. Leonidov and L. McLerran, *Nucl.Phys.* **A692** (2001) 583;
E. Ferreiro, E. Iancu, A. Leonidov and L. McLerran, *Nucl. Phys.* **A 701** (2002) 489;
E. Iancu and R. Venugopalan, hep-ph/0303204.

[5] J. Jalilian-Marian, A. Kovner, A. Leonidov and H. Weigert, *Nucl. Phys.* **B 504** (1997) 415; *Phys. Rev.* **D 59** (1999) 014014. J. Jalilian-Marian, A. Kovner and H. Weigert, *Phys. Rev.* **D 59** (1999) 014015.

[6] A.H. Mueller, *Phys. Lett.* **B 523** (2001) 243.

[7] I. I. Balitsky, *Nucl. Phys.* **B463** (1996) 99; *Phys. Rev. Lett.* **81** (1998) 2024; *Phys. Rev.* **D60** (1999) 014020; *Phys. Lett.* **B518** (2001) 235;
I.I. Balitsky and A.V. Belitsky, *Nucl. Phys.* **B 629** (2002) 290.

[8] H. Weigert, *Nucl. Phys.* **A 703** (2002) 823.

[9] J. Bartels and M. Wüsthoff, *Z. Phys.* **C66** (1995) 157.

[10] Yu. V. Kovchegov, *Phys. Rev.* **D60** (1999) 034008.

[11] A. H. Mueller, *Nucl. Phys.* **B415** (1994) 373;
A.H. Mueller and B. Patel, *Nucl. Phys.* **B 425** (1994) 471.

[12] Yu. V. Kovchegov, *Phys. Rev.* **D61** (2000) 074018.

[13] E. M. Levin and K. Tuchin, *Nucl. Phys.* **B573** (2000) 833; *Nucl.Phys.* **A691** (2001) 779; *Nucl. Phys.* **A693** (2001) 787.

[14] M. A. Braun, *Eur. Phys. J.* **C16** (2000) 337; `hep-ph/0010041`;
N. Armesto and M. A. Braun, *Eur. Phys. J.* **C20** (2001) 517.

[15] E. Gotsman, E.M. Levin, M. Lublinsky and U. Maor, *Nucl. Phys.* **A 696** (2001) 851; M. Lublinsky, *Eur. Phys. J.* **C21** (2001) 513.

[16] K. Golec-Biernat, L. Motyka, A.M. Staśto, *Phys. Rev.* **D** (2002) 074037.

[17] S. Bondarenko, M. Kozlov and E. Levin, `hep-ph/0305150`.

[18] M. Froissart, *Phys. Rev.* **123** (1961) 1053; A. Martin, *Phys. Rev.* **129** (1963) 1432.

[19] A. Kovner and U.A. Wiedemann, *Phys. Rev.* **D 66** (2002) 051502; *Phys. Rev.* **D 66** (2002) 034031; *Phys. Lett.* **B 551** (2003) 311.

[20] E. Ferreiro,E. Iancu, K. Itakura and L. McLerran, *Nucl. Phys.* **A 710** (2002) 373.

[21] N. N. Nikolaev and B. G. Zakharov, *Z. Phys.* **C 49**(1991) 607; *Z. Phys.* **C 53**(1992) 331.

[22] L. N. Lipatov,*Sov. Phys. JETP* **63** (1986) 904.

[23] G.P. Salam, *Nucl. Phys.* **B 449** (1995) 589; *Nucl. Phys.* **B 461** (1996) 512.

[24] G. P. Salam, *Comput. Phys. Commun.* **105** (1997) 62.

[25] J. Bartels and E. Levin, *Nucl.Phys.* **B387** (1992) 617.

[26] A. M. Staśto, K. Golec-Biernat and J. Kwieciński, *Phys. Rev. Lett.* **86** (2001) 596.

[27] K. Golec–Biernat and M. Wüsthoff, *Phys. Rev.* **D59** (1999) 014017; *Phys. Rev.* **D60** (1999) 114023; *Eur. Phys. J.* **C20** (2001) 313.

[28] G. Bottazzi, G. Marchesini, G.P. Salam and M. Scorletti, *Nucl. Phys.* **B 505** (1997) 366.

[29] R.J. Glauber, *Phys. Rev.* **100** (1955) 242.

[30] A. H. Mueller *Nucl. Phys.* **B 335** (1990) 115.

[31] K. Golec-Biernat and A.M. Staśto, work in progress.

[32] E. Iancu, K. Itakura and L. McLerran, *Nucl. Phys.* **A 708** (2002) 327.

[33] A.H. Mueller and D.N. Triantafyllopoulos, *Nucl. Phys.* **B 640** (2002) 331.

[34] V. S. Fadin, M. I. Kotsky and R. Fiore, *Phys. Lett.* **B 359**, 181 (1995);
V. S. Fadin, M. I. Kotsky and L. N. Lipatov, BUDKERINP-96-92, `hep-ph/9704267`;
V. S. Fadin, R. Fiore, A. Flachi and M. I. Kotsky, *Phys. Lett.* **B 422**, 287 (1998);
V. S. Fadin and L. N. Lipatov, *Phys. Lett.* **B 429**, 127 (1998);
G. Camici and M. Ciafaloni, *Phys. Lett.* **B 386**, 341 (1996); *Phys. Lett.* **B 412**, 396 (1997) [Erratum-ibid. B **417**, 390 (1997)]; *Phys. Lett.* **B 430**, 349 (1998).

[35] S. Munier, S. Wallon, `hep-ph/0303211`.

[36] M.G. Ryskin, talk on DIS2003 conference.

[37] A.H. Mueller, *Nucl. Phys.* **B 437** (1995) 107.

[38] W. Heisenberg, *Z. Phys.* **133**, (1952) 65.